

Application of novel photocatalytic and adsorption fibers in water treatment

Ya-Fei Yang

Department of Occupational Safety and Health Chung Hua University of Medical Technology, No. 89, Wenhua 1st St., Rende Dist., Tainan City 717, Taiwan, ROC, email: cillia55@gmail.com

Received 9 October 2021; Accepted 5 April 2022

ABSTRACT

Photocatalysts and adsorption material are used in several processes including the destruction of organic pollutants in drinking water treatment. Although titanium dioxide and zeolite are considered as powerful, adsorbent, radical producers, their particles are small, making particle separation difficult. In this research, a novel process to immobilize catalyst particles to aid particle recovery is developed, and its efficacy in removing organic pollutants in water is evaluated. The process involves the impregnation of titanium dioxide and zeolite particles into hollow fibers made from polyvinylidene fluoride (PVDF), forming both photocatalytic hollow fibers (PCHF) and photocatalytic adsorption hollow fibers (PCDHF). Dimethylacetamide (DMAc) was used as the solvent, and water was used as an external coagulant during spinning of the PCHF. The PCHF were synthesized at different PVDF/TiO₂ and DMAc/water ratios, respectively. As indicated in the experimental results, both nitrobenzene (NB) and *Microcystis* were degraded by the developed PCHF. At a fiber dose of 0.4 g/L, NB was degraded from 80 to 32 mg/L within 90 min. The process followed second-order kinetics to nitrobenzene (NB) and hydroxyl radicals with a rate constant of 5.0×10^{-9} M/s and hydroxyl radical concentration of 1.74×10^{-12} mol/L. 1 g of zeolite (Hisiv 6000) can adsorb about 10 mg of ammonium nitrate. Although further research is still needed, this study demonstrates that the developed PCHF and PCDHF can produce radicals and increase treatment efficiency, and therefore could be applied to remove organic pollutants from water.

Keywords: Titanium dioxide; Hollow fibers; Radicals; Oxidation; Photocatalyst; Adsorption

1. Introduction

Water is vital to human life [1]. Water reservoirs are the most important source of public water supply globally, as rivers and stream levels are inconsistent [2,3]. However, the influx of large amounts of nitrogen and phosphorus nutrients in recent years has caused eutrophication to become increasingly serious, resulting in the frequent appearance of algal blooms in many reservoirs. These present potential risks of toxins and undesirable odors in the public water supply, as well as complicating water treatment and increasing water usage risks [4,5]. An influx of algae causes toxicity in reservoir raw water areas after its rupture and death. However, the biggest risk is at the water supply

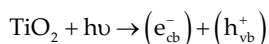
terminal where chlorine is often added as a disinfectant. Chlorine destroys algae, subsequently producing toxins and carcinogenic N-nitrosamines [6]. Currently there is no effective method for inhibiting or degrading algae toxins and N-nitrosamines in water sources or terminal water supplies. Moreover, when raw water containing a large amount of nutrients is introduced into industrial water, several of the nutrients, including nitrogen and phosphorus [5], are regarded as reusable resources. Discharging nutrient-rich wastewater into the natural environment leads to a weakening of the ecosystem, and the consequent ammonium nitrate problem will not only appear in domestic water but also in industrial wastewater, thus causing serious water pollution [7].

Nitrates (especially ammonia) are essential to human life, but excessive wastewater discharge containing these nutrients causes environmental problems [8,9]. It is necessary to remove ammonia from wastewater to avoid potential environmental pollution and reduce conventional ammonia production to reduce greenhouse gas emissions [10].

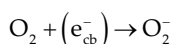
TiO₂ photocatalysis is becoming an increasingly interesting oxidation process in air cleaning as well as water treatment. In water purification, its main advantage is the ability to completely mineralize organics due to the photo-generation of OH• radicals in water via the OH groups on the TiO₂ surface [11,12]. The principle of photocatalysis is simple; namely a catalyst harnesses (UV) radiation energy from sunlight to break down different substances. Photocatalysis can break down a variety of organic materials, including organic acids, estrogens, pesticides, dyes, crude oil, microbes (including viruses and chlorine resistant organisms), inorganic molecules such as nitrous oxides (NOx), and can also remove mercury and heavy metals through precipitation or filtration. However, some disadvantages also persist. For instance, the separation of fine particles is a slow and expensive process as the UV light penetration is limited due to the strong TiO₂ adsorption and dissolved organic species. Some researchers have attempted to minimize these problems by immobilizing TiO₂ on various materials such as glass plates [13], porous glass [14], tubes [15], zeolite [16], and fiberglass mesh [17–19].

Under UV ($\lambda < 390$ nm), it is highly reactive with a band gap above 3–3.2 eV, and thus, optically stimulated electrons (e⁻) in the conduction band and electric holes (h⁺) in the valence electron band may be generated. After excitation from the valence band to the conduction band, free holes may be produced in the valence band. Photo-generated electrons contribute to the generation of reactive oxygen species (ROS), resulting in photocatalyst reactions that enhance photocatalytic degradation, while e⁻ and h⁺ react with H₂O and O₂ adsorbed on the surface of TiO₂, forming active groups including OH and O₂⁻. In addition, TiO₂ possesses a high capacity for oxidative decomposition and forms super hydrophilicity as a chemical phenomenon due to relevant reactions. However, TiO₂ photocatalysis has some inherent disadvantages, which limit the TiO₂ efficiency during photocatalytic processes. Furthermore, UV is used to irradiate TiO₂ as the corresponding band gap is about 3.2 eV. The TiO₂ photocatalytic efficiency is not high enough in sunlight containing only about 5% UV light [19–21]. The photocatalytic reaction mechanism is as follows [21]:

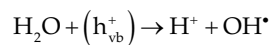
- When photocatalysts are excited by light, electron-hole pairs ($h\nu \geq E_g = 3.2$ eV) form.



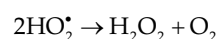
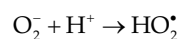
- Electrons and oxygen molecules adsorbed on the surface form superoxide molecules.



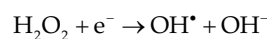
- Electric hole oxidizes the water molecules adsorbed on the surface to form hydroxyl radicals.



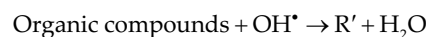
- Hydrogen peroxide is produced in the process.



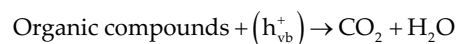
- Hydrogen peroxide forms hydroxyl radicals.



- After continuous attacks by hydroxyl radicals, the organic compounds are oxidized.



- Organic compounds directly oxidize with the electric hole.



In this study, nitrogen-modified titanium dioxide is introduced to promote photosensitivity. Doping with non-metals is conducted for two reasons: (1) to lower the titanium dioxide energy gap by raising the valence electron band, or form extra holes by adding non-metals with a different valency, thus reducing the bonding of electron hole pairs; (2) to change titanium dioxide physical properties such as its surface area and pore size. Moreover, some studies have directly modified titanium dioxide, so as to reduce its energy gap, enhance its reaction ability, and increase its reaction rate [22,23].

Among organic polymer materials, polyvinylidene fluoride (PVDF) is commonly used in ultrafiltration (UF), microfiltration (MF), and pervaporation (PV) membrane manufacturing processes due to its excellent thermal stability and chemical resistance to aggressive reagents including organic solvents, acids, and bases [24]. The obtained PVDF membranes are characterized by good tensile strength and an asymmetric separation structure. Pure PVDF membrane is susceptible to contamination by proteins and other impurities during water and wastewater treatment, resulting in a sharp drop in its water flux [25]. Although its hydrophobic nature promotes the selective adsorption and transport of organic components in an organic/water feed solution, the neat PVDF membrane is liable to contamination of proteins and other impurities in the process of water and wastewater treatment, leading to a sharp drop in pure water flux of the membrane [26]. There have been several studies on improving

PVDF membrane performance including utilizing physical blending, chemical grafting, and surface modification [27,28]. Among these methods, the polymer blending has the advantage of easy phase-inversion preparation.

TiO₂ has received significant attention owing to its stability, availability, and application potential in the fields of painting, catalysis and photocatalysis, batteries, and cosmetics, etc. In water treatment, TiO₂ is often used as a photocatalyst to accelerate the degradation of organic contaminants. When dispersed into PVDF membrane, TiO₂ nanoparticles improve the hydrophilicity of the membranes, enhance the flux, and facilitate the photocatalytic degradation of several organic compounds [29].

In this research, titanium dioxide was selected as the research material. Titanium dioxide has photocatalytic reaction characteristics, stable chemical properties, is non-toxic and cheap. Under ultraviolet light, it can convert light energy into chemical energy, release hydroxyl radicals with high oxidizing ability (OH[•]) and degrade and mineralize water pollutants. However, the oxidizing ability of most TiO₂ is only activated ultraviolet photocatalysis, which is not only energy-consuming but also disadvantageous to its application. In view of this, nitrogen atom-doped modified titanium dioxide (N-doped TiO₂) was also used in this study to facilitate catalysis to increase oxidizing ability under visible light, enabling field application [30]. In practice, applying TiO₂ as a catalyst is problematic as its particles are tiny, difficult to disperse in solution, and challenging to recycle, which can easily cause secondary pollution. Therefore, in this study, titanium dioxide was combined with hollow fiber to create a new material. Using titanium dioxide powder, allows it to be completely and uniformly dispersed on the fiber structure and surface. This greatly increases the contact area and mass transfer rate and also allows the materials to be reused. The novel photocatalytic hollow fibers (PCHF) developed in this research can be specifically designed with a suitable ratio and type according to varying water quality and pollutants, which improves the treatment efficiency.

Removal and recovery of ammonia from wastewater has always been a major issue globally, and is key to realizing a sustainable nitrogen cycle and circular economy. Air stripping is a comprehensive method available for the direct simultaneous removal and recovery of ammonium nitrate from wastewater using chemical additives to adjust the pH in advance. By using a photocatalyst for catalysis and hollow fiber for adsorption, chemical use can be avoided [31–33]. Zeolites are used as ion exchange agents, adsorbents, catalysts, desiccants, molecular sieves, fertilizers, soil enrichment agents, etc. Some specific zeolites have a high adsorption and ion exchange capacity, ion exchange selectivity, catalytic activity, and structural stability up to 700°C–750°C [31–34]. With hydrophilic surfaces, regularly arranged molecular level pores, and the capacity for cation exchange, zeolites are good adsorbents of metal ions, catalysts, and organic compounds. Zeolites also have a high selectivity and treatment efficiency for ammonium nitrate pollution [35]. After adsorption saturation, the zeolites can be regenerated using a sodium chloride or potassium chloride solution. The regeneration

solution is then treated with sodium hypochlorite, which may cause nitrogen to escape from the ammonium nitrate. The zeolites may also be regenerated following adsorption saturation at 350°C–650°C for reuse [36–38].

Adsorption and catalysis technologies are the most common ways to remove and concentrate organic and inorganic pollutants in water but have many issues such as unsatisfactory treatment effects, high cost, and excessive waste due to a limited reaction contact area and overall low mass transfer rate. The aim of this study, was to use the large surface area and porosity of hollow fibers, as well as catalysts, to resolve the reaction area and mass transfer resistance issues. As a result, the fibers could be used in water treatment materials and technology to improve water treatment efficiency while reducing cost and waste [39,40].

However, regardless of whether titanium dioxide or zeolite powder is used as the water treatment agent, secondary pollution caused by the fine powders chosen for the high surface area, is not the only consideration. Therefore, this study presents a new treatment technology for immobilizing such powders to guarantee treatment efficiency. The technology is simple and convenient to use without any secondary pollution. Photocatalytic hollow fibers (PCDHFs) can realize a multi-effective treatment after zeolites are added to the photocatalytic fibers as adsorbents. With both photocatalysis and adsorption effects, PCDHFs are more suited to practical use.

2. Experimental materials

The photocatalytic material used for the hollow fibers was TiO₂ P25, purchased from Degussa, and polyvinylidene fluoride (PVDF) was used as the polymer. N,N-dimethylacetamide (DMAc) was used to prepare the polymer solution. Distilled water was used as an internal coagulant and tap water was used as the external coagulant.

The photocatalytic material for the hollow fibers was TiO₂ P25 purchased from Degussa, and N-doped titanium dioxide powder. The ammonium nitrate adsorption material was synthesized using Hisiv zeolite powder (USKY-79, Hisiv1000, Hisiv3000, and Hisiv6000).

The N-doped titanium dioxide powder was synthesized by titanium(IV) isopropoxide and melamine via the sol-gel process. The sol-gel process can be divided into the following steps: (1) hydrolysis and condensation polymerization, (2) gelation, (3) aging, (4) drying, and (5) thermal treatment. The principle is basically as follows: metal inorganic salt and pure salt are used as precursors to compel the solvent and solute to undergo hydrolysis or alcoholysis; forming a sol in the mixing process; finally, the sol is dried, obtaining a dry powder.

N,N-dimethylacetamide (DMAc) was used as the solvent during the polymer dope preparation. Firstly, the required quantity of organic solvent (DMAc) was added to a 1 or 0.5 L wide-neck bottle and the desired quantity of polymer (PVDF) was then slowly added. Secondly, the bottle was placed on a rotary pump to stir the mixture and form the polymer solution. After a clear polymer solution was formed, the appropriate amount of titanium dioxide powder was added, and the mixture was stirred for 24 h to ensure thorough dispersion. This is essential in

the spinning process as aggregates can lead to successful spinning and blocking of the spinning dye.

2.1. Spinning of photocatalytic hollow fibers

The polymer solution was transferred to a stainless-steel container and degassed for 24 h at room temperature before spinning. This ensured that any gas bubbles were completely removed from the polymer solution. The pressure was set as 2–3 bar, using nitrogen, during spinning. The hollow fiber spinning system is shown in Fig. 1.

Photocatalytic hollow fiber was produced using a spinneret, into which polymer dope was fed via nitrogen gas, then passed through an adjustable air gap before entering a quench bath. Tap water was used as an environmentally friendly and easily available quench bath medium. The fiber was then passed through a coagulation bath and collected on a fiber tank. Care was taken to ensure continuity of the pressure and internal water support in order to avoid any trapped air or fiber separation to ensure successful spinning.

Subsequently, the hollow fibers were soaked in fresh water for 1–2 d, to ensure thorough removal of any residual solvent.

2.2. Characterization and performance evaluation

Scanning electron microscopy (SEM) was used to characterize the surface and profile of the photocatalytic hollow fiber. The surface structure was observed using a Hitachi S3000-N model, while the fiber performance was observed using an Agilent 1260 UPLC. Titanium dioxide was activated and compared under UV light at 256 and 365 nm wavelengths. Nitrobenzene (NB) and p-chlorobenzoic acid (p-CBA) were used when determining the hydroxyl radicals, since OH^\bullet radicals could not be measured directly during oxidation, and nitrobenzene has recently been used as an OH^\bullet radical probe compound.

2.3. Recycling of photocatalytic hollow fibers and photocatalytic adsorption hollow fibers

The photocatalytic hollow fibers (PCDHF) degrade pollutants mainly by the photocatalytic reaction of electronic holes for titanium dioxide. Theoretically, there is no consumption. The main reason why the degradation efficiency is reduced during the application process is that the PCDHF surfaces are blocked by organic pollutant coating, and thus, the area available for photoreaction is reduced. Relevant regeneration methods are employed to remove organics on the surface with sodium hypochlorite disinfectant (0.5 mol/L).

The photocatalytic adsorption hollow fibers PCDHFs produce hydroxyl radicals which degrade organics in water via photocatalysis, and realize wastewater ammonium nitrate adsorption due to the high specific surface area of porous zeolites. After adsorption saturation, PCDHFs are cleaned with 10% hydrochloric acid for desorption, and ammonium chloride is obtained after crystallization of the desorption agent. The cleaned PCDHFs can then be recycled.

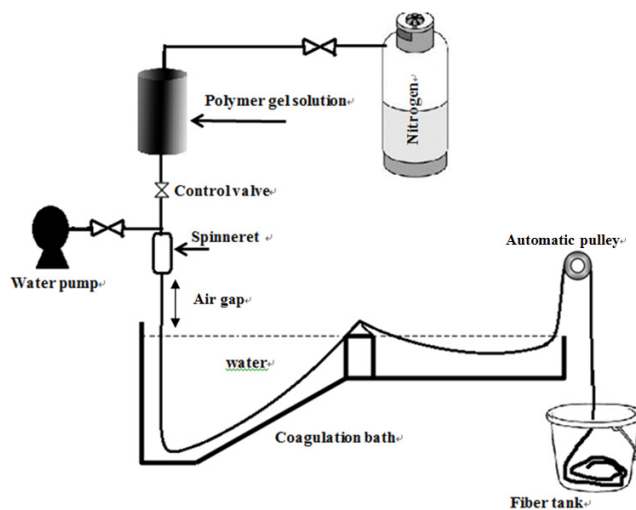


Fig. 1. Photocatalytic hollow fiber spinning system.

3. Result and discussion

X-ray diffraction (XRD) was used for a characteristic analysis and detailed investigation of the crystal image and lattice size changes of modified titanium dioxide under different conditions. During the study, eight titanium dioxide powders were prepared with different nitrogen content, under different calcination temperatures. The molar ratios of nitrogen to titanium/calcination temperatures for the powders were 0% 400°C, 0% 500°C, 15% 400°C, 15% 500°C, 20% 400°C, 20% 500°C, 25% 400°C, and 25% 500°C, respectively. The XRD analysis results, presented in Fig. 2A and B, indicate that with molar ratios of nitrogen to titanium of 0%, 15%, 20%, and 25%, the titanium dioxide lattice size at a calcination temperature of 400°C was about 40%–50% smaller than at 500°C. At the same time, there were several correlations between the crystal phase and titanium lattice size; (1) The smaller the lattice size, the larger the specific surface area, and the higher the excitation effect of the hydroxyl radicals after light absorption; (2) The band gaps of the anatase and rutile crystal phases were roughly 3.2 and 3 eV, respectively; (3) The anatase crystal phase photoactivity was better than that of the rutile crystal phase. Therefore, the titanium dioxide effect at 400°C was predicted to be better than at 500°C. In addition, for modified and unmodified titanium dioxide at a calcination temperature of 400°C, only 15% of the nitrogen-modified titanium dioxide exhibited a crystal phase transformation from anatase to rutile, while the excitation of rutile occurred more readily than for anatase.

Fig. 3A and B show the SEM micrographs of photocatalytic hollow fiber prepared with about 30 wt.% TiO_2 . The pore size ranged from 0.5 to 3.0 μm . The TiO_2 nanoparticles were deposited on the surface and inner pores of the PVDF hollow fiber, as shown in Fig. 4A and B.

Fig. 5A illustrates the results of nitrobenzene photodegradation by photocatalytic hollow fiber. As shown, probe compound nitrobenzene rapidly degraded in the initial 10 min, then the reaction rate slowed down. Fig. 5 also shows that the removal efficiency using solid

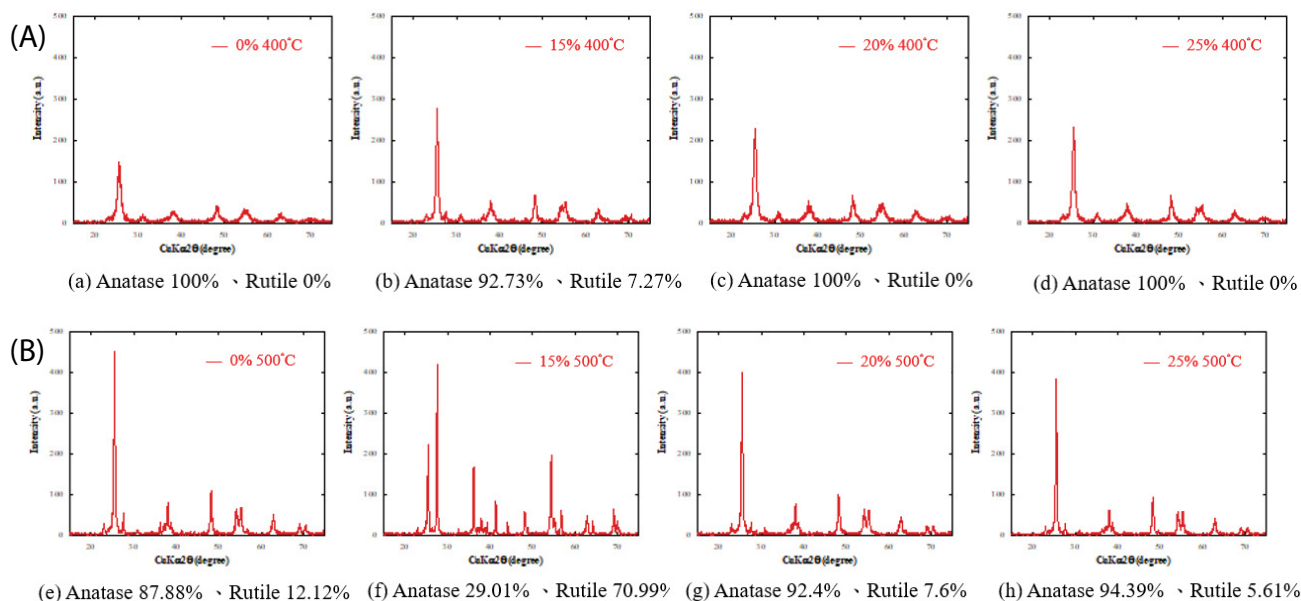


Fig. 2. XRD results of nitro-modified titanium dioxide powders with different molar ratios of nitrogen to titanium, at a calcination temperature of (A) 400°C and (B) 500°C.

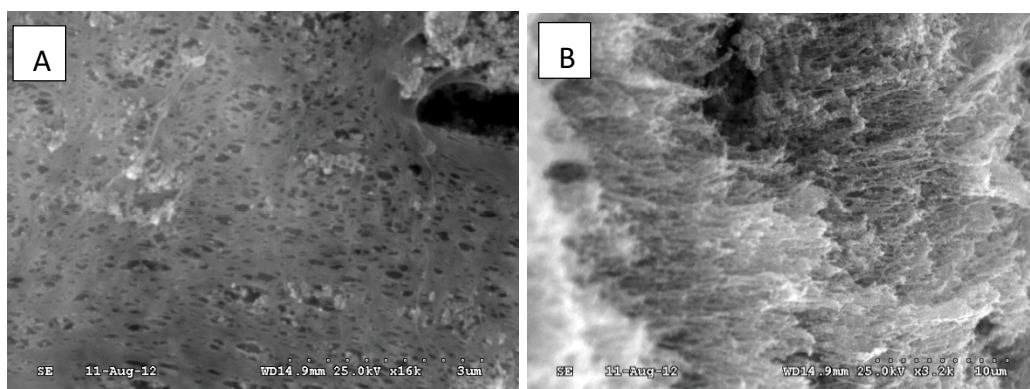


Fig. 3. (A) (PVDF/DMAc, 20/80) photocatalytic hollow fiber (Surface SEM) and (B) (PVDF/DMAc, 20/80) photocatalytic hollow fiber (Profile SEM).

photocatalytic fiber is higher than when using TiO_2 powder; the photocatalytic hollow fiber specific surface area and hydroxyl radical burst size are higher than those of the TiO_2 powder. Fig. 5B shows the different ratios for polymer and DMAc, where the optimum condition is at a ratio of 20:80 (polymer/DMAc).

The application mainly focuses on using sunlight as the photocatalyst activation light source. Therefore, sunlight was used as the light source in this experiment. Six samples of titanium dioxide powder, prepared under different conditions, were added to p-CBA solution with a concentration of about 5 mg/L; the sampling interval was 2 h, and the experiment lasted for about 6 h. The purpose was to explore the degradation of p-CBA under sunlight at the same time. The initial pH value for the experiment was 7.0, and remained constant throughout the experiment. The experimental parameters are as shown in Table 1.

The p-CBA integral area of the sample was tested by high performance liquid chromatography (HPLC), then converted into p-CBA concentration on the basis of “Fig. 6 Calibration curves of the concentration and integral area of p-CBA”. In addition, the changes in p-CBA concentration of the six samples were obtained, as shown in Fig. 6.

Fig. 6 presents the degradation of p-CBA by titanium dioxide, modified under different conditions. The fitted line shows the reaction kinetic rates obtained under the assumed first-order degradation condition. As clearly demonstrated in the figure, the p-CBA degradation degree of titanium dioxide, modified under different conditions, is ranked as follows: 15% 400°C > 20% 400°C > 25% 400°C > 20% 500°C > 25% 500°C > 15% 500°C. The degradation kinetic parameters are summarized in Table 1, and reveal that the reaction kinetic rate can be increased 5–10 times under the optimum modification conditions. As clearly observed

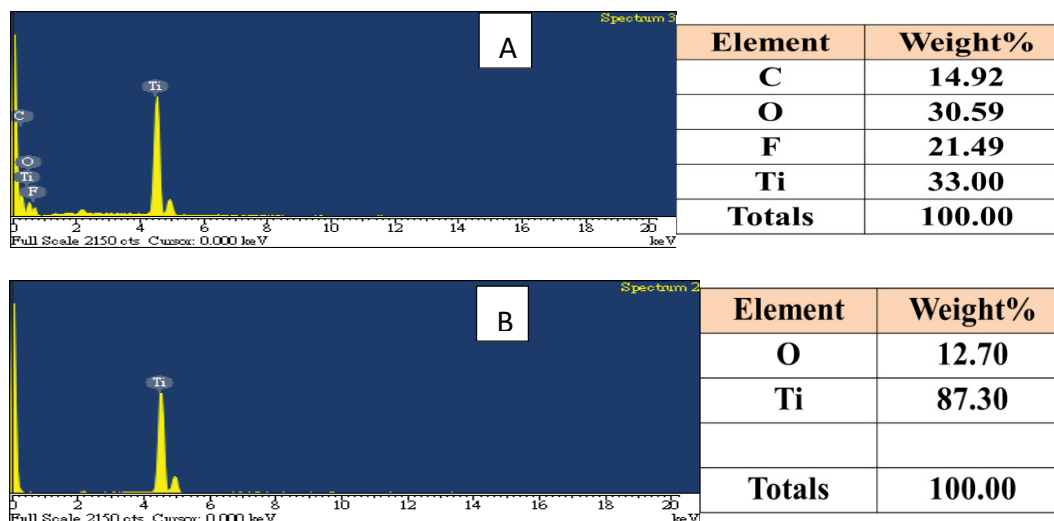


Fig. 4. (A) (PVDF/DMAc, 20/80) photocatalytic hollow fiber (Surface EDS) and (B) (PVDF/DMAc, 20/80) photocatalytic hollow fiber (Profile EDS).

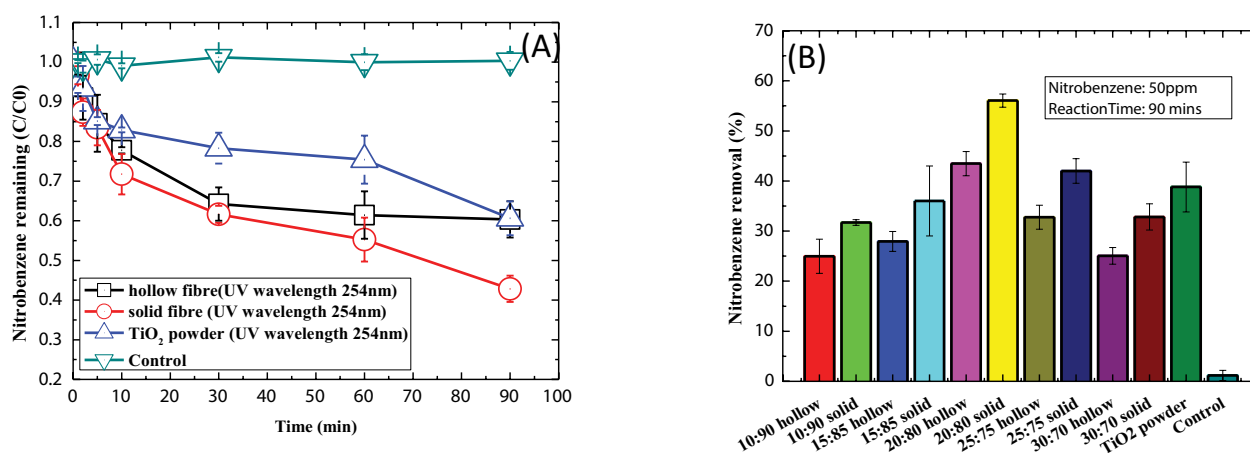


Fig. 5. Results of nitrobenzene photodegradation by photocatalytic hollow fiber: (A) the removal efficiencies by using TiO_2 powder and photocatalytic hollow fiber and (B) different ratios (polymer/DMAc).

Table 1
 OH^\bullet kinetic rate constant

Condition	Kinetic rate constant (S^{-1})	R^2
15% 400°C	2.1×10^{-4}	0.998
15% 500°C	1.6×10^{-5}	0.692
20% 400°C	1.7×10^{-4}	0.999
20% 500°C	5.8×10^{-5}	0.972
25% 400°C	1.5×10^{-4}	0.998
25% 500°C	5.8×10^{-5}	0.925

from the reaction kinetic rate constants in Fig. 6 and Table 1, the modification effect at a calcination temperature of 500°C is inferior to that at 400°C (approximately 50% less). Nevertheless, for the N-doped titanium dioxide powder calcinated at 400°C, the best reaction effect was

obtained under the conditions of 15% 400°C as the p-CBA was almost fully degraded during 6h of sunlight irradiation.

Fig. 7 demonstrates that N-doped titanium dioxide can effectively activate OH^\bullet under visible light (Fig. 7A). When hydroxyl radicals exist in natural water, they can suppress algal growth. In terms of the correlation between cell integrity and algal toxins, photocatalytic fibers can destroy algae cells and effectively inhibit the generation of algal toxins (Fig. 7B). When algae in natural water reacts with hydroxyl radicals, algae cells are destroyed by oxidization, releasing algal toxins. Meanwhile, the algal toxins are rapidly degraded by the hydroxyl radicals, hence realizing the inhibition of algal growth.

Zeolite can adsorb ammonium nitrate to some extent. The experimental results show that Hisiv6000 (Fig. 8A) performs the best. However, its performance is significantly influenced by the calcination temperature during the manufacturing process. When the calcination

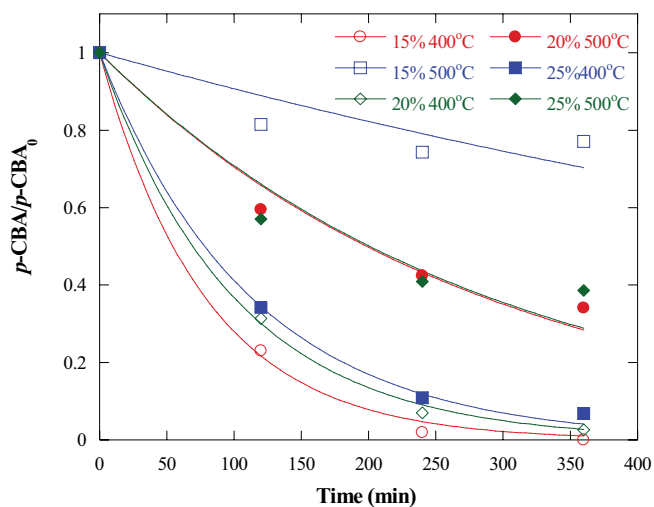


Fig. 6. OH• kinetics of reaction (p-CBA).

temperature is increased to 400°C, its adsorption capacity is several times that of zeolite calcinated at 100°C. Meanwhile, optimized conditions are conducive to the adsorption of ammonium nitrate. 1 g of zeolite can adsorb about 10 mg of ammonium nitrate, which increases as the calcination temperature rises.

We have attempted to create a double-layer hollow fiber structure to achieve both photocatalysis and adsorption. The organic matter adsorbed in the column can be efficiently further oxidized by photocatalyst. When using a zeolite and titanium dioxide compound under ultraviolet light, the titanium dioxide activates hydroxyl radicals and oxidizes the ammonium nitrate organic substances. Subsequently, the remaining ammonium nitrate can be adsorbed by Hisiv 6000 zeolite. This enables the almost total degradation of ammonium nitrate, as shown in Fig. 9.

4. Conclusion

PVDF-titanium hollow fiber was successfully prepared by spinning PVDF and DMAc fixed TiO₂ photocatalytic

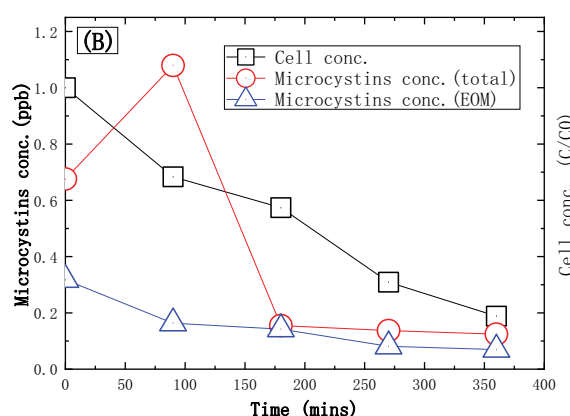
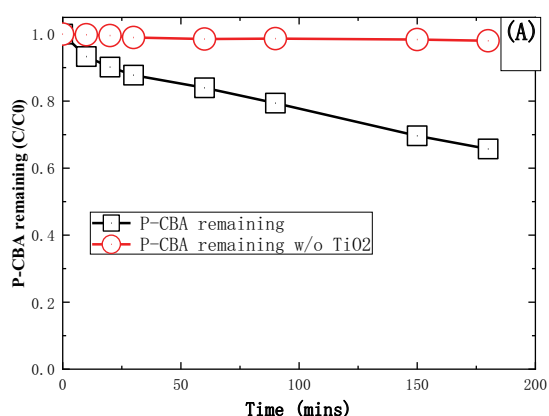


Fig. 7. Visible light test on environmental algal toxin (using N-doped photocatalytic fibre) (A) Test on the performance of N-doped titanium dioxide photocatalytic fibre. (B) Test on cell integrity and microcystin degradation (Total: cell body contains extracellular substances; EOM: extracellular organic substance does not contain cell body).

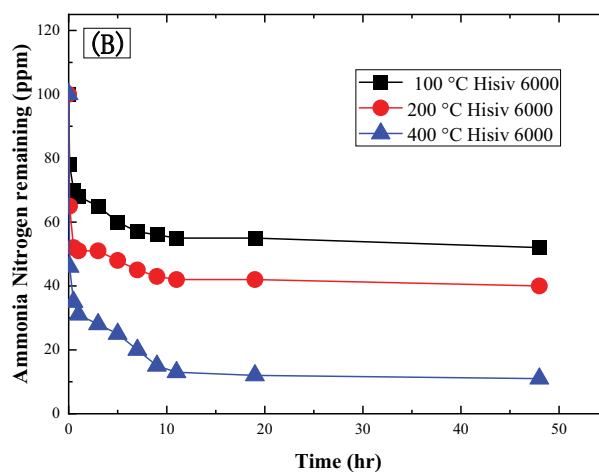
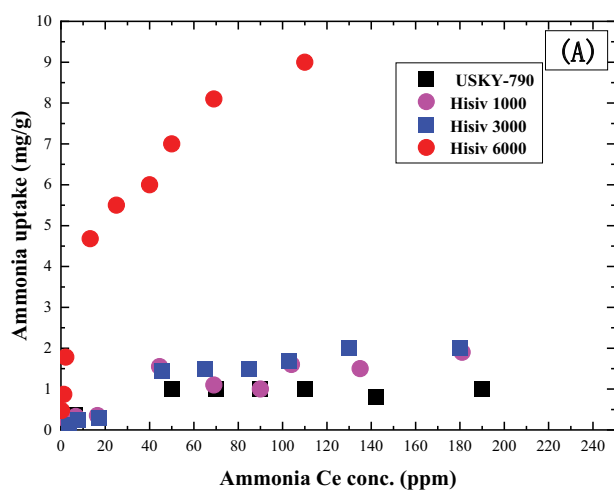


Fig. 8. Test on the ammonia nitrogen adsorption performance of zeolite.

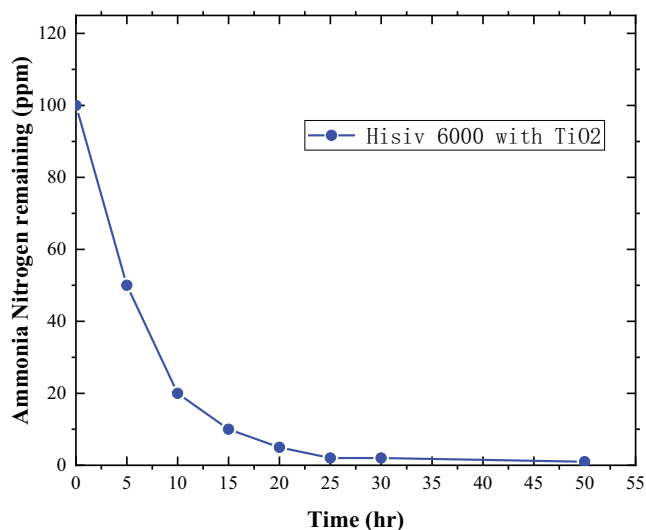


Fig. 9. Test on the ammonia nitrogen degradation performance of zeolite and TiO₂ mixed photocatalytic fibre.

hollow fiber, achieving an increased hydroxyl radical burst size rate and specific surface area. Through experimental analysis, it was confirmed that fixed titanium dioxide in photocatalytic hollow fiber demonstrated a higher removal efficiency of organic compounds in water, and the photocatalytic hollow fiber was more easily recycled. In addition, the NB removal efficiency as directly proportional to the titanium dioxide content in the hollow fibers, and the efficiency under UV with a wavelength of 254 nm was better than with a wavelength of 365 nm. The research results demonstrate that the developed PCHF can produce radicals and therefore can be applied in removing organic pollutants during water treatment.

For the treatment of ammonium nitrate, we compared four adsorbent materials (USKY-790, Hisiv1000, Hisiv3000, and Hisiv6000). In the synthesis of adsorption hollow fibers, the adsorption efficiency of Hisiv6000 was >85% after forging at 400°C. In this study, we used the hollow fiber's ability to create a two-layer structure, by integrating TiO₂ photocatalysis and zeolite adsorption into the same hollow fiber to achieve simultaneous adsorption and oxidation in a single column, which not only improves the treatment efficiency, but improves its applicability in actual plant treatment.

Data availability statement

All relevant data is included in the paper or in its Supplementary Information.

References

- P.-E. Persson, Off-flavours in aquatic ecosystems – an introduction, *Water Sci. Technol.*, 15 (1983) 6–7.
- P.-M. Kao, B.-M. Hsu, T.-K. Hsu, Y.-C. Chiu, C.-L. Chang, W.-T. Ji, S.-W. Huang, C.-W. Fan, Application of TaqMan qPCR for the detection and monitoring of *Naegleria* species in reservoirs used as a source for drinking water, *Parasitol. Res.*, 113 (2014) 3765–3771.
- C.-H. Chang, L.-Y. Cai, T.-F. Lin, C.-L. Chung, L. Van der Linden, M. Burch, Assessment of the impacts of climate change on the water quality of a small deep reservoir in a humid-subtropical climatic region, *Water*, 7 (2015) 1687–1711.
- A.P. Davis, M. Shokouhian, H. Sharma, C. Minami, Water quality improvement through bioretention media: nitrogen and phosphorus removal, *Water Environ. Res.*, 78 (2006) 284–293.
- J. Kim, J.R. Jones, D. Seo, Factors affecting harmful algal bloom occurrence in a river with regulated hydrology, *J. Hydrol.: Reg. Stud.*, 33 (2021) 100769, doi: 10.1016/j.ejrh.2020.100769.
- C.-C. Fan, T.-F. Lin, N-nitrosamines in drinking water and beer: detection and risk assessment, *Chemosphere*, 200 (2018) 48–56.
- D. Li, X. Xu, Z. Li, T. Wang, C. Wang, Detection methods of ammonia nitrogen in water: a review, *TrAC, Trends Anal. Chem.*, 127 (2020) 115890, doi: 10.1016/j.trac.2020.115890.
- R. Xu, Y. Cai, X. Wang, C. Li, Q. Liu, Z. Yang, Agricultural nitrogen flow in a reservoir watershed and its implications for water pollution mitigation, *J. Cleaner Prod.*, 267 (2020) 122034, doi: 10.1016/j.jclepro.2020.122034.
- M.M. Aldaya, C.I. Rodriguez, A. Fernandez-Poulussen, D. Merchan, M.J. Beriain, R. Llamas, Grey water footprint as an indicator for diffuse nitrogen pollution: the case of Navarra, Spain, *Sci. Total Environ.*, 698 (2020) 134338, doi: 10.1016/j.scitotenv.2019.134338.
- A. Beckinghausen, M. Odlare, E. Thorin, S. Schwede, From removal to recovery: an evaluation of nitrogen recovery techniques from wastewater, *Appl. Energy*, 263 (2020) 114616, doi: 10.1016/j.apenergy.2020.114616.
- J. Singh, S. Sharma, A.S. Basu, Synthesis of Fe₂O₃/TiO₂ monoliths for the enhanced degradation of industrial dye and pesticide via photo-Fenton catalysis, *J. Photochem. Photobiol., A*, 376 (2019) 32–42.
- J.C. Garcia, J.L. Oliveira, A.E.C. Silva, C.C. Oliveira, J. Nozaki, N.E. de Souza, Comparative study of the degradation of real textile effluents by photocatalytic reactions involving UV/TiO₂/H₂O₂ and UV/Fe²⁺/H₂O₂ systems, *J. Hazard. Mater.*, 147 (2007) 105–110.
- C.-F. Lo, J.C.S. Wu, Preparation and characterization of TiO₂-coated optical-fiber in a photo reactor, *J. Chin. Inst. Chem. Eng.*, 36 (2005) 119–126.
- C.J. Pestana, J. Portela Noronha, J. Hui, C. Edwards, H.Q. Nimal Gunaratne, J.T.S. Irvine, P.K.J. Robertson, J. Capelo-Neto, L.A. Lawton, Photocatalytic removal of the cyanobacterium *Microcystis aeruginosa* PCC7813 and four microcystins by TiO₂ coated porous glass beads with UV-LED irradiation, *Sci. Total Environ.*, 745 (2020) 141154, doi: 10.1016/j.scitotenv.2020.141154.
- S. Bao, H. Liang, C. Li, J. Bai, A heterostructure BiOCl nanosheets/TiO₂ hollow-tubes composite for visible light-driven efficient photodegradation antibiotic, *J. Photochem. Photobiol., A*, 397 (2020) 112590, doi: 10.1016/j.jphotochem.2020.112590.
- J.G. Piedra López, O.H. González Pichardo, J.A. Pinedo Escobar, D.A. de Haro del Río, H. Inchaurregui Méndez, L.M. González Rodríguez, Photocatalytic degradation of metoprolol in aqueous medium using a TiO₂/natural zeolite composite, *Fuel*, 284 (2021) 119030, doi: 10.1016/j.fuel.2020.119030.
- M. Penpolcharoen, R. Amal, M. Brungs, Degradation of sucrose and nitrate over titania coated nano-hematite photocatalysts, *J. Nanopart. Res.*, 3 (2001) 289–302.
- S. Moeini Najafabadi, F. Rashidi, M. Rezaei, Performance of a multistage rotating mesh support photoreactor immobilized with TiO₂ on photocatalytic degradation of PNP: reactor construction and optimization, *Chem. Eng. Process. Process Intensif.*, 146 (2019) 107668, doi: 10.1016/j.cep.2019.107668.
- Y.-H. Li, S.-W. Cheng, C.-S. Yuan, T.-F. Lai, C.-H. Hung, Removing volatile organic compounds in cooking fume by nano-sized TiO₂ photocatalytic reaction combined with ozone oxidation technique, *Chemosphere*, 208 (2018) 808–817.
- N.T.-T. Hoang, A.T.-K. Tran, T.-A. Le, D.D. Nguyen, Enhancing efficiency and photocatalytic activity of TiO₂-SiO₂ by combination of glycerol for MO degradation in continuous reactor under solar irradiation, *J. Environ. Chem. Eng.*, 9 (2021) 105789, doi: 10.1016/j.jece.2021.105789.
- J. Ge, Z. Zhang, Z. Ouyang, M. Shang, P. Liu, H. Li, X. Guo, Photocatalytic degradation of (micro)plastics using

- TiO₂-based and other catalysts: properties, influencing factor, and mechanism, *Environ. Res.*, 209 (2022) 112729, doi: 10.1016/j.envres.2022.112729.
- [22] B. Ayoubi-Feiz, M.H. Mashhadizadeh, M. Sheydaei, Degradation of diazinon by new hybrid nanocomposites N-TiO₂/Graphene/Au and N-TiO₂/Graphene/Ag using visible light photo-electro catalysis and photo-electro catalytic ozonation: optimization and comparative study by Taguchi method, *Sep. Purif. Technol.*, 211 (2019) 704–714.
- [23] K. Rajeshwar, M.E. Osugi, W. Chanmanee, C.R. Chenthamarakshan, M.V.B. Zaroni, P. Kajitvichyanukul, R. Krishnan-Ayer, Heterogeneous photocatalytic treatment of organic dyes in air and aqueous media, *J. Photochem. Photobiol., C*, 9 (2008) 171–192.
- [24] L. Wu, J. Sun, Q. Wang, Poly(vinylidene fluoride)/polyethersulfone blend membranes: effects of solvent sort, polyethersulfone and polyvinylpyrrolidone concentration on their properties and morphology, *J. Membr. Sci.*, 285 (2006) 290–298.
- [25] X. Cao, J. Ma, X. Shi, Z. Ren, Effect of TiO₂ nanoparticle size on the performance of PVDF membrane, *Appl. Surf. Sci.*, 253 (2006) 2003–2010.
- [26] S.P. Dharupaneedi, S.K. Nataraj, M. Nadagouda, K.R. Reddy, S.S. Shukla, T.M. Aminabhavi, Membrane-based separation of potential emerging pollutants, *Sep. Purif. Technol.*, 210 (2019) 850–866.
- [27] Y. Ma, X. Chen, S. Wang, H. Dong, X. Zhai, X. Shi, J. Wang, R. Ma, W. Zhang, Significantly enhanced antifouling and separation capabilities of PVDF membrane by synergy of semi-interpenetrating polymer and TiO₂ gel nanoparticles, *J. Ind. Eng. Chem.*, 108 (2021) 15–27.
- [28] L. Yan, Y.S. Li, C.B. Xiang, S. Xianda, Effect of nano-sized Al₂O₃-particle addition on PVDF ultrafiltration membrane performance, *J. Membr. Sci.*, 276 (2006) 162–167.
- [29] C.S. Ong, W.J. Lau, P.S. Goh, B.C. Ng, A.F. Ismail, Investigation of submerged membrane photocatalytic reactor (sMPR) operating parameters during oily wastewater treatment process, *Desalination*, 353 (2014) 48–56.
- [30] M.C. Ortega-Liébana, J.L. Hueso, S. Ferdousi, K.L. Yeung, J. Santamaria, Nitrogen-doped luminescent carbon nanodots for optimal photo-generation of hydroxyl radicals and visible-light expanded photo-catalysis, *Diamond Relat. Mater.*, 65 (2016) 176–182.
- [31] H. Huang, B. Li, J. Dai, W. Wang, M. Zhang, Y. Ou, Ammonia nitrogen removal from coking wastewater and high quality gypsum recovery by struvite recycling by using calcium hydroxide as decomposer, *J. Environ. Manage.*, 292 (2021) 112712, doi: 10.1016/j.jenvman.2021.112712.
- [32] F. Ulu, M. Kobya, Ammonia removal from wastewater by air stripping and recovery struvite and calcium sulphate precipitations from anesthetic gases manufacturing wastewater, *J. Water Process Eng.*, 38 (2020) 101641, doi: 10.1016/j.jwpe.2020.101641.
- [33] A. Folino, D.A. Zema, P.S. Calabrò, Organic matter removal and ammonia recovery by optimised treatments of swine wastewater, *J. Environ. Manage.*, 270 (2020) 110692, doi: 10.1016/j.jenvman.2020.110692.
- [34] L. Kumar, R. Kaur, J. Sharma, The efficiency of zeolites in water treatment for combating ammonia – an experimental study on Yamuna River water & treated sewage effluents, *Inorg. Chem. Commun.*, 134 (2021) 108978, doi: 10.1016/j.inoche.2021.108978.
- [35] A.A. Halim, H.A. Aziz, M.A.M. Johari, K.S. Ariffin, Comparison study of ammonia and COD adsorption on zeolite, activated carbon and composite materials in landfill leachate treatment, *Desalination*, 262 (2010) 31–35.
- [36] S.M. Muscarella, L. Badalucco, B. Cano, V.A. Laudicina, G. Mannina, Ammonium adsorption, desorption and recovery by acid and alkaline treated zeolite, *Bioresour. Technol.*, 341 (2021) 125812, doi: 10.1016/j.biortech.2021.125812.
- [37] M. Zhao, D. Ma, Y. Ye, Adsorption, separation and recovery properties of blocky zeolite-biochar composites for remediation of cadmium contaminated soil, *Chin. J. Chem. Eng.*, (2021), doi: 10.1016/j.cjche.2021.10.020 (In Press).
- [38] J. Probst, J.G. Outram, S.J. Couperthwaite, G.J. Millar, P. Kaparaju, Sustainable ammonium recovery from wastewater: improved synthesis and performance of zeolite N made from kaolin, *Microporous Mesoporous Mater.*, 316 (2021) 110918, doi: 10.1016/j.micromeso.2021.110918.
- [39] A.M. Awad, R. Jalab, A. Benamor, M.S. Nasser, M.M. Ba-Abbad, M. El-Naas, A.W. Mohammad, Adsorption of organic pollutants by nanomaterial-based adsorbents: an overview, *J. Mol. Liq.*, 301 (2020) 112335, doi: 10.1016/j.molliq.2019.112335.
- [40] W. Hu, Y. Xie, S. Lu, P. Li, T. Xie, Y. Zhang, Y. Wang, One-step synthesis of nitrogen-doped sludge carbon as a bifunctional material for the adsorption and catalytic oxidation of organic pollutants, *Sci. Total Environ.*, 680 (2019) 51–60.